

# Structure and Morphology of Polyamide 66 and Oligomeric Phenolic Resin Blends: Molecular Modeling and Experimental Investigations

Juha Hartikainen,<sup>\*,†</sup> Olli Lehtonen,<sup>§</sup> Tapio Harmia,<sup>†</sup> Mathias Lindner,<sup>†</sup> Sami Valkama,<sup>§</sup> Janne Ruokolainen,<sup>§</sup> and Klaus Friedrich<sup>‡</sup>

*FACT Future Advanced Composites and Technology GmbH, Hertelsbrunnenring 9, D-67657 Kaiserslautern, Germany, Institut für Verbundwerkstoffe GmbH, Erwin-Schrödinger-Strasse Geb. 58, D-67663 Kaiserslautern, Germany, and Department of Engineering Physics and Mathematics and Center for New Materials, Helsinki University of Technology, P.O. Box 2200, FIN-02015 HUT, Espoo, Finland*

*Received February 27, 2004. Revised Manuscript Received May 12, 2004*

Interaction between polyamide 66 (PA66) and phenol formaldehyde resin (PFR) was studied by molecular modeling for oligomeric model compounds and by experimental methods. Complexation between *N*-methylacetamide (NMA) and phenol was analyzed by calculating the equilibrium structure, hydrogen bond length, and interaction energy. Additionally, electrostatic potential (ESP) derived atomic charges were computed. Quantum mechanical calculations combined with an experimental Fourier transform infrared spectroscopy (FTIR) study revealed that there exists a strong hydrogen bonding between the carbonyl group of NMA and the hydroxyl group of phenol. Furthermore, the interaction energy of the NMA–phenol complex was found to exceed that of the NMA and phenol dimers and also their complexes with water molecules, which provides an explanation for the decreased water absorption of polyamides upon blending with PFR. FTIR and differential scanning calorimetry (DSC) studies of PA66–PFR blends demonstrated, in addition, miscible blends with hydrogen bond connections between the components. Furthermore, microscopic analyses by optical polarization microscope and transmission electron microscope (TEM) revealed that PFR induced spherulite growth in PA66.

## Introduction

Aliphatic polyamides are widely used semicrystalline polymers, characterized by their excellent mechanical performance combined with good resistance to chemicals. The properties of these materials also remain at the same level over a wide temperature scale ranging from sub-zero to 150 °C. These are the underlying factors that have made aliphatic polyamides as one of the most successful class of plastic materials in the market, the most important commercial types being polyamide 6 (PA6) and polyamide 66.<sup>1</sup> During recent years, several attempts to modify aliphatic polyamides in order to further improve mechanical performance or to achieve new desirable properties have been published in the literature, one of the most studied methods being blending of PA with other thermoplastic polymers or rubbers.<sup>2–4</sup> Large number of possible variations in blends leads to a very broad range of properties, which

has made blending a popular modification method also in industrial scale.

Blending of various thermoplastics with phenol based thermosets has recently attained attention as an alternative route to achieve new property combinations. The driving force for the miscibility in these blends is a strong hydrogen bonding formed between the hydroxyl group of a phenolic resin (donor) and the functional group of a thermoplastic counterpart (acceptor).<sup>5</sup> Poly(methyl methacrylate) (PMMA) was one of the first polymers that was noticed to form miscible blends with oligomeric phenol formaldehyde resins.<sup>5,6</sup> By crosslinking of the thermoset counterpart it was possible to even achieve interpenetrating network (IPN) type structures, though only when PFR was rich in composition.<sup>7,8</sup> In the PMMA-rich region it is not possible to achieve a thermoset network structure over the whole material, for which reason phase separation takes place upon curing, especially if the cross-linking density is high.<sup>8</sup> Similarly, miscible blends between PFR and a variety of other thermoplastics have been reported, including poly(vinyl acetate),<sup>5</sup> ethylene-vinyl acetate copoly-

\* To whom correspondence should be addressed.

† FACT Future Advanced Composites and Technology GmbH.

‡ Institut für Verbundwerkstoffe GmbH.

§ Helsinki University of Technology.

(1) Kohan, M. I. *Nylon Plastics Handbook*; Hanser/Gardner Publications: Cincinnati, 1995.

(2) Paul, D. R.; Bucknall, C. B., Eds. *Polymer Blends*; John Wiley & Sons: USA, 1999.

(3) Collyer, A. A., Ed. *Rubber Toughened Engineering Plastics*; Chapman & Hall: Cambridge, 1994.

(4) Utracki, L. A., Ed. *Polymer Blends Handbook*; Kluwer Academic Publishers: Dordrecht, Netherlands, 2002.

(5) Fahrenholtz, S. R.; Kwei, T. K. *Macromolecules* **1981**, *14*, 1076.

(6) Pennacchia, J. R.; Pearce, E. M.; Kwei, T. K.; Bulkin, B. J.; Chen, J.-P. *Macromolecules* **1986**, *19*, 973.

(7) Kim, H.-I.; Pearce, E. M.; Kwei, T. K. *Macromolecules* **1989**, *22*, 3374.

(8) Zhang, X.; Solomon, D. H. *Macromolecules* **1994**, *27*, 4919.

mers,<sup>9,10</sup> poly( $\epsilon$ -caprolactone),<sup>11</sup> and poly(adipic ester).<sup>12</sup> In recent reports it was demonstrated that PFR and poly(2-vinylpyridine)-polystyrene and poly(2-vinylpyridine)-poly(isoprene) block-copolymers form miscible blends with self-organized spherical, cylindrical, and lamellar nanostructures.<sup>13,14</sup> Also, various polyamides have been blended with PFR type thermosets recently, showing miscibility due to the hydrogen bonding between hydroxyl group of phenolic resin and carbonyl group of amide functionality.<sup>15–19</sup>

In light of recent publications it seems that the addition of PFR affects both the crystalline and amorphous phases of semicrystalline polymers, which in turn may be reflected in final properties of the blends. Recently Huang and co-workers<sup>18,19</sup> studied the morphological changes in PA6 blended with poly(4-vinyl phenol) and with oligomeric, chlorinated novolac-type phenolic resin, concluding that phenol containing counterparts locate largely in amorphous phase. This assumption is based on small-angle X-ray scattering (SAXS) patterns, indicating that the thickness of the crystalline layer is essentially unchanged upon blending. In another study it was observed that a small amount of oligomeric novolac-type PFR induced the spherulite growth rate in PA6. The size of the spherulites increased compared to neat PA6, but the nucleation density decreased simultaneously.<sup>17</sup> In the same study it was noticed that the dynamic tensile modulus of the blends was higher compared to PA6, possibly due to the decreased water absorption of the blends. It can be also considered whether the higher modulus originates from the changes in crystalline structure or from the hydrogen bonding “cross-link” network in PA6-PFR blends.

In the present study we attempt to bring more understanding of the structure of polyamide-PFR blends by a systematic study for model compounds and for the corresponding macromolecular system. To investigate interactions between polyamide and phenolic resins and the effect of water on the structure and morphology of polyamide, adequate model molecules were chosen to make quantum mechanical calculations. *N*-methyl acetamide and phenol molecules were taken to represent polyamide and PFR, respectively. Also, the experimental FTIR spectrum of the complex is presented and discussed. The modeling results are compared to FTIR, DSC, and microscopy studies for PA66-PFR blends. It can be considered whether such a blend is a route to a reduced water uptake, improved stability and enhanced

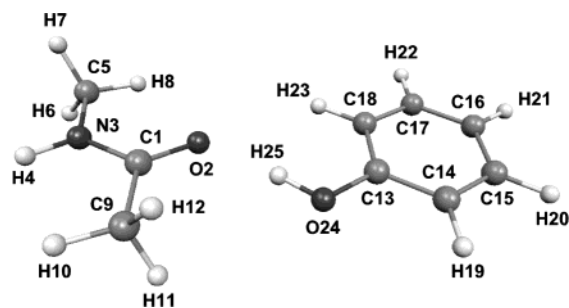


**Figure 1.** Chemical structure and labeling of atoms in *N*-methylacetamide-phenol complex.

mechanical performance of PA66, and similar commodity polyamides.

## Experimental Section

**Materials.** *N*-methylacetamide (NMA) and phenol were of 99% purity and supplied by Aldrich, see Figure 1 for the structures. Zytel PA66 of DuPont was provided in granulate form by Biesterfeld Plastics GmbH (Germany) and its viscosity averaged molecular weight  $M_v$  was 32 700 g/mol, as analyzed by the solution viscosity method in concentrated sulfuric acid. Phenolic formaldehyde resin was of type Supraplast 1763 and provided by Süd-West-Chemie GmbH (Germany). It was a novolac-type phenolic resin having a weight averaged molecular weight  $M_w$  of 989 g/mol and a number averaged molecular weight  $M_n$  of 463 g/mol as analyzed by gel permeation chromatography.

**Sample Preparation.** The NMA-phenol complex was directly mixed in a molar ratio of 1:1 at 30 °C by a magnetic stirrer for 4 h. The sample was stored in a vacuum desiccator before FTIR analysis. To prepare the polymer blends, powdered phenol formaldehyde resin was mechanically mixed with PA66 granulates at ratios varying from 0 to 50 wt % of PFR in PA66. After mixing, the blends were melt processed by using a Haake Buchler Rheocord System 40 laboratory scale twin screw extruder. The temperature profile was set to 240–290 °C and the screw speed was 40 rpm. After processing, the blend samples were left to cool slowly to room temperature, dried overnight in a vacuum oven at 60 °C, and stored in a vacuum desiccator until analyzed.

**Modeling.** All calculations were done using Gaussian 03 program<sup>20</sup> running on an SGI Origin 2000 computer system. The computational methods used were density functional theory (DFT) with a hybrid functional B3LYP<sup>21</sup> and the second-order Møller-Plesset perturbation theory (MP2). Geometry optimizations of all molecules were done using B3LYP/6-31+G(d,p) level of theory; the standard 6-31+G(d,p) basis set including polarization functions on all elements and diffuse functions on all non-hydrogen elements. Energies at the optimized geometries were calculated using MP2/6-31+G(d,p), B3LYP/6-31+G(d,p), and B3LYP/6-311++G(2df,p) methods, the standard 6-311++G(2df,p) basis set involving two d and

(9) Coleman, M. M.; Serman, C. J.; Painter, P. C. *Macromolecules* **1987**, *20*, 226.

(10) Mekhilef, N.; Hadjiandreou, P. *Polymer* **1995**, *36*, 2165.

(11) Zhong, X.; Guo, Q. *Polymer* **1997**, *38*, 279.

(12) Ma, C.-C. M.; Wu, H.-D.; Chu, P. P.; Tseng, H.-T. *Macromolecules* **1997**, *30*, 5443.

(13) Kosonen, H.; Ruokolainen, J.; Nyholm, P.; Ikkala, O. *Polymer* **2001**, *42*, 9481.

(14) Kosonen, H.; Ruokolainen, J.; Nyholm, P.; Ikkala, O. *Macromolecules* **2001**, *34*, 3046.

(15) Yang, T. P.; Pearce, E. M.; Kwei, T. K.; Yang, N. L. *Macromolecules* **1989**, *22*, 1813.

(16) Wang, F.-Y.; Ma, C.-C. M.; Hung, A. Y. C.; Wu, H.-D. *Macromol. Chem. Phys.* **2001**, *202*, 2328.

(17) Huang, M. W.; Zhu, K. J.; Pearce, E. M.; Kwei, T. K. *J. Appl. Polym. Sci.* **1993**, *48*, 563.

(18) Huang, P. T.; Lee, J. L.; Chiu, S. C.; Kwei, T. K.; Pearce, E. M. *J. Appl. Polym. Sci.* **1999**, *73*, 295.

(19) Huang, P.-T.; Kwei, T. K.; Pearce, E. M.; Levchik, S. V. *J. Polym. Sci., Part A: Polym. Chem.* **2001**, *39*, 841.

(20) Frisch, M. J.; Trucks, G. W.; Schlegel, H. B.; Scuseria, D. E.; Robb, M. A.; Cheeseman, J. R.; Montgomery, J. A.; Vreven, T. J.; Kudin, K. N.; Burant, J. C.; J. M. Millam, J. M.; Iyengar, S. S.; Tomasi, J.; Barone, V.; Mennucci, B.; Cossi, M.; Scalmani, G.; Rega, N.; Petersson, G. A.; Nakatsuji, H.; Hada, M.; Ehara, M.; Toyota, K.; Fukuda, R.; Hasegawa, J.; Ishida, M.; Nakajima, T.; Honda, Y.; Kitao, O.; Nakai, H.; Klene, M.; Li, X.; Knox, J. E.; Hratchian, H. P.; Cross, J. B.; Adamo, C.; Jaramillo, J.; Gomperts, R.; Stratmann, R. E.; Yazyev, O.; Austin, A. J.; Cammi, R.; Pomelli, C.; Ochterski, J. W.; Ayala, P. Y.; Morokuma, K.; Voth, G. A.; Salvador, P.; Dannenberg, J. J.; Zakrzewski, V. G.; Dapprich, S.; Daniels, A. D.; Strain, M. C.; Farkas, O.; Malick, D. K.; Rabuck, A. D.; Raghavachari, K.; Foresman, J. B.; Ortiz, J. V.; Cui, Q.; Baboul, A. G.; Clifford, S.; Cioslowski, J.; Stefanov, B. B.; Liu, G.; Liashenko, A.; Piskorz, P.; Komaromi, I.; Martin, R. L.; Fox, D. J.; Keith, T.; Al-Laham, M. A.; Peng, C. Y.; Nanayakkara, A.; Challacombe, M.; Gill, P. M. W.; Johnson, B.; Chen, W.; Wong, M. W.; Gonzalez, C.; Pople, J. A. *Gaussian 03*, Revision B.02.; Gaussian, Inc.: Pittsburgh, PA, 2003.

(21) Becke, A. D. *J. Chem. Phys.* **1993**, *98*, 5648.

one *f* type polarization functions on all non-hydrogen elements and *p* type polarization functions on hydrogens and diffuse functions on all elements. Basis set superposition error was estimated using the counterpoise correction<sup>22,23</sup> with the 6-31+G(d,p) basis set for both B3LYP and MP2 methods. Electrostatic potential (ESP) derived atomic charges were also calculated, using the CHelpG method.<sup>24</sup>

**FTIR.** A Nicolet 510 FTIR spectrometer was used to analyze hydrogen bonding in model compounds and in polymer blends. Model compounds NMA, phenol, and NMA(phenol)<sub>1.0</sub> complex were either mixed and pelletized within KBr (phenol) or “sandwiched” between two KBr pellets (NMA and complex). Polymer blend samples were ground in powder form together with KBr and then pressed to pellets. Minimum number of scans was 32 with a resolution of 4 cm<sup>-1</sup>.

**DSC.** A Mettler Toledo DSC 821 device was used to determine glass transition and melting temperatures of the blends. The samples were first heated to 270 °C and then cooled back to room temperature to equalize thermal histories. *T<sub>g</sub>* and *T<sub>m</sub>* values were taken from the second heating scan. The rate of the heating and cooling was 10 °C/min.

**Transmission Electron Microscopy (TEM).** Ultrathin sections (approximately 100 nm) of PA66/PFR blends for TEM characterization were microtomed at room temperature using a Leica Ultracut UCT ultramicrotome and a Diatome-diamond knife. Bright-field TEM was performed for unstained films on JEOL-1200EX transmission electron microscope operating at an accelerating voltage of 60 kV.

**Optical Microscopy.** Films of PA66/PFR blends were cut by using Leitz 1400 microtome. Film thicknesses of 25–30 μm was used. The films were analyzed by using Leitz Diaplan polarization microscope equipped with video camera.

## Results and Discussion

**Calculations.** Analysis of the fine chemical structure of polymer systems is a relatively complex matter, especially if quantum mechanical calculations are considered. By using oligomeric model compounds including similar functionalities as in corresponding polymeric system, it is possible to mimic changes taking place, for example, in the blending of two dissimilar polymers. Recently it was demonstrated in the context of conducting polymer polyaniline complexed with dodecylbenzenesulfonic acid (DBSA) and Zinc(DBSA)<sub>2</sub> salt that by using a model compound approach it is possible to round the complexity of the corresponding macromolecular system, leading to detailed information about the crystalline structures.<sup>25</sup> Similarly, quantum mechanical calculations for pyridine complexed with methane sulfonic acid gave a new insight to the protonation of conjugated polymers with sulfonic acids.<sup>26</sup> Also, an interassociation equilibrium constant in PA6-phenolic resin blend was recently estimated by using *N*-propylacetamide complexed with 2,4-xylenol.<sup>16</sup> These examples show that modeling with low molecular weight analogues offers a convenient route for detailed structure analysis.

In the present work we have used *N*-methylacetamide as a model for polyamide and phenol as a model for phenol formaldehyde resin. NMA and phenol were

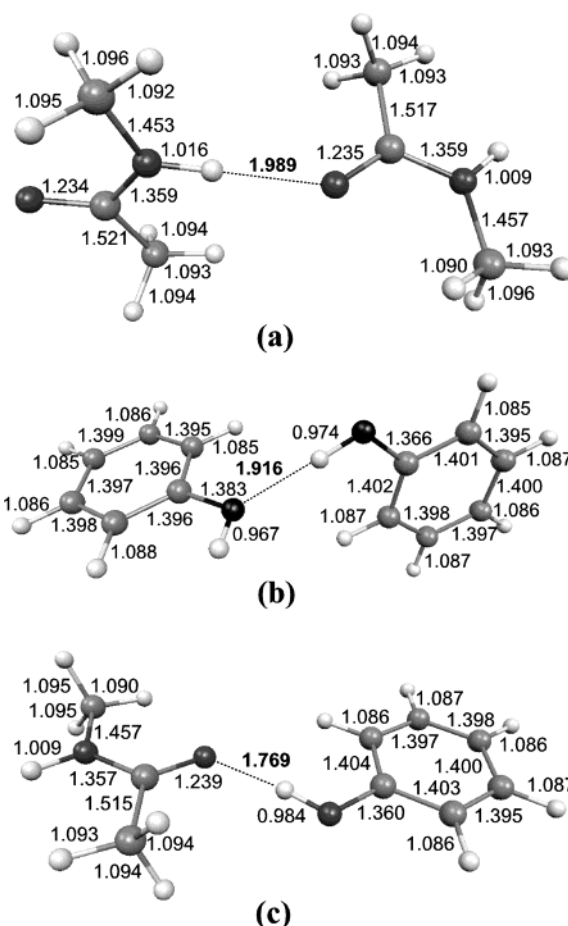


**Figure 2.** Optimized structure and calculated bond lengths in (a) *N*-methylacetamide dimer, (b) phenol dimer, and (c) *N*-methylacetamide-phenol complex.

chosen due to their simple structures, which allowed quantum chemical calculations to be performed using DFT and MP2 levels of theory. Optimized geometries and hydrogen bonding energies for the phenol dimer, NMA dimer, and NMA-phenol complex were calculated. Additionally, inspired by the fact that water molecules have a strong effect on mechanical properties of various polar thermoplastics, as well as on polymer chain degradation via hydrolysis reaction, hydrogen bonding in water-NMA and water-phenol complexes was investigated. In the case of NMA, hydrogen bonding with water molecules takes place essentially through CO (acceptor) or through NH (donor) functionalities of NMA. Similarly, in the case of phenol, water can be hydrogen bonded either directly to a hydroxyl oxygen (acceptor) or a hydroxyl proton (donor). These possibilities were analyzed by calculating the interaction energies.

Calculated minimum energy structures for NMA dimer, phenol dimer, and NMA-phenol complex are shown in Figures 2a–c and the complexation energies by MP2/6-31+G(d,p) and B3LYP/6-31+G(d,p) methods are given in Table 1. Although no systematic conformation search for the molecules was performed, the most obvious conformations were initially examined; both 180° and 0° conformations of NMA, with respect to the torsion angle formed by O–C–N–H, were optimized by the B3LYP/6-31G+(d,p) method. It was found that the 180° conformation was energetically more favorable by 9.8 kJ/mol. Calculations by the B3LYP/6-311++G(2df,p)

(22) Boys, S. F.; Benardi, F. *Mol. Phys.* **1970**, *19*, 553.

(23) van Duijneveldt, F. B.; van Duijneveldt-van de Rijdt, J. G. C. M.; van Lenthe, J. H. *Chem. Rev.* **1994**, *94*, 1873.

(24) Breneman, C. M.; Wiberg, K. B. *J. Comput. Chem.* **1990**, *11*, 361.

(25) Hartikainen, J.; Lahtinen, M.; Torckeli, M.; Serimaa, R.; Valkonen, J.; Rissanen, K.; Ikkala, O. *Macromolecules* **2001**, *34*, 7789.

(26) Lehtonen, O.; Hartikainen, J.; Rissanen, K.; Ikkala, O.; Pietilä, L.-O. *J. Chem. Phys.* **2002**, *116*, 2417.

**Table 1. Complexation Energies, Estimated Basis Set Superposition Errors (BSSE) and Calculated Counterpoise Corrected Complexation Energies (unit kJ/mol) in *N*-methylacetamide Dimer, Phenol Dimer, and *N*-methylacetamide-phenol Complex by B3LYP/6-31+G(d,p) and MP2/6-31+G(d,p) Methods**

molecules	donor	acceptor	method 1: B3LYP/6-31+G(d,p)			method 2: MP2/6-31+G(d,p)			
			$\Delta E_1$	BSSE1	$\Delta E_1$ corr.	$\Delta E_2$	BSSE2	$\Delta E_1$ corr.	
NMA dimer	N	H	O (NMA)	-27.3	1.4	-25.9	-38.1	6.9	-31.2
phenol dimer	O	H	O (phenol)	-22.6	3.4	-19.2	-34.6	10.6	-24.0
NMA-phenol	O	H	O (NMA)	-40.0	2.3	-37.7	-47.5	8.8	-38.8
NMA-water	O	H	O (NMA)	-32.5	2.0	-30.4	-35.2	6.2	-29.0
NMA-water	N	H	O (water)	-21.6	3.4	-18.2	-27.6	7.7	-19.9
phenol-water	O	H	O (phenol)	-18.2	2.3	-15.9	-23.4	6.2	-17.2
phenol-water	O	H	O (water)	-30.9	4.8	-26.1	-35.7	9.9	-25.8

method were also carried out, giving similar values as B3LYP/6-31+G(d,p), which indicates that the use of simpler basis set with counterpoise correction is justified. Thus, only the corrected values of MP2 and B3LYP with the 6-31+G(d,p) basis set are considered in the following discussion. It can be seen that in the minimum energy structure of the NMA-phenol complex (Figure 2c), there exists a hydrogen bonding between the carbonyl oxygen of NMA and hydroxyl proton of phenol. Both methods predicted that hydrogen bond strength is highest in the NMA-phenol complex and weakest in the phenol dimer, whereas in the NMA dimer the strength is between these two, as evidenced by the differences in calculated, counterpoise corrected complexation energies: -26 to -31 kJ/mol for the NMA dimer, -19 to -24 kJ/mol for the phenol dimer but -38 to -39 kJ/mol for NMA-phenol complex. The results indicate that NMA and phenol form a stable complex with a dissociation energy exceeding that of the dimers. Additionally, it can be noticed from the values of Table 1 that one of the NMA-water complexes (CO...H) has a complexation energy of comparable magnitude to that of NMA dimer, enabling water molecules to break the intermolecular hydrogen bonds between NMA monomers and to form a strong physical bonding with amide moieties. B3LYP/6-31+G(d,p) predicts the difference between NMA dimer and NMA-water (CO...H) to be about 4.5 kJ/mol in favor of the NMA-water but MP2/6-31+G(d,p) gives a value of 2.2 kJ/mol in favor of NMA dimer. Differences between the values given by DFT and MP2 are most probably due to the dispersion interactions which are to some extent included in MP2 but not properly accounted for by DFT. On the other hand, the hydrogen bond strength is 8 to 10 kJ/mol higher in the NMA-phenol complex than in the NMA-water complex, which suggests that the phenolic group could actually protect amide moieties from water. The same phenomenon is also reflected by the bond lengths between the monomers. Optimized geometries of the complexes (Figure 2) show that the hydrogen bond length is 1.989 Å in the case of NMA dimer and 1.916 Å in the case of phenol dimer. However, the calculated hydrogen bond length for the NMA-phenol complex is only 1.769 Å, which again suggests that there exists a strong interaction between NMA and phenol, exceeding that of the dimers.

These results can be linked to macromolecular systems including amide functionalities. Water absorption and hydrolysis reactions in polyamides occur essentially in an amorphous region,<sup>27</sup> though erosion of the crystal-

line phase may take place at elevated temperature.<sup>28</sup> It is obvious that unbonded amide groups become connected with water molecules first, but it has been suggested that eventually amide-amide hydrogen bonds of amorphous region may also be replaced by bonding with water, upon treatment of the samples in humid conditions.<sup>27</sup> Calculations for the model compounds carried out in the present study show that the complexation energy of the amide-amide hydrogen bond is close to the energy of the amide-water hydrogen bond, which indicates that disruption of hydrogen bonds between polyamide chains may indeed take place. It is known that if polyamides are blended with oligomers such as phenol formaldehyde resin including high amount of hydroxyl groups that can bond with amide, water absorption decreases.<sup>17</sup> Although water is still able to break intermolecular hydrogen bonds between amide groups in this system, phenolic resins are able to form a network that binds different polymer chains together via hydrogen bonding. Due to the strong interaction between amide and hydroxyl groups, water is unable to break these hydrogen bonds to a large extent.

Figures 3a and 3b show the calculated atomic charges of NMA dimer and NMA-phenol complex. The charges are also collected in Table 2. It can be seen that there is a change in charge of the carbonyl carbon of NMA (C1) from 0.655 in the NMA dimer to 0.613 in the complex with phenol. In the context of polyamide it is known that the carbonyl carbon is prone to the attack of water molecules, leading to a polymer chain degradation and loss of mechanical properties. Now, if the charge of the carbonyl carbon is decreased, a consequence is that the reactivity of the amide group with water is reduced. In a polymeric system this means that polyamide complexed with a phenol-type group would have a decreased tendency towards hydrolysis reaction. Thus, it is suggested that oligomers or polymers containing phenolic groups may also protect polyamide against hydrolysis. However, it must be noted that the hydrogen bond density decreases after the temperature is increased above the glass transition temperature ( $T_g$ ) in such blends,<sup>6</sup> which restricts the concept to temperatures below  $T_g$ .

**Experimental Verification.** Fourier transform infrared spectra (FTIR) of NMA, phenol, and NMA-phenol complex were measured at room temperature, to study whether the complexation takes place similarly to the calculated minimum energy state proposed; that is, if there exists a hydrogen bonding between a carbonyl group of NMA and a hydroxyl group of phenol. Figure

(27) Murthy, N. S.; Stamm, M.; Sibilja, J. P.; Krimm, S. *Macromolecules* **1989**, *22*, 1261.

(28) Chaupart, N.; Serpe, G.; Verdu, J. *Polymer* **1998**, *39*, 1375.

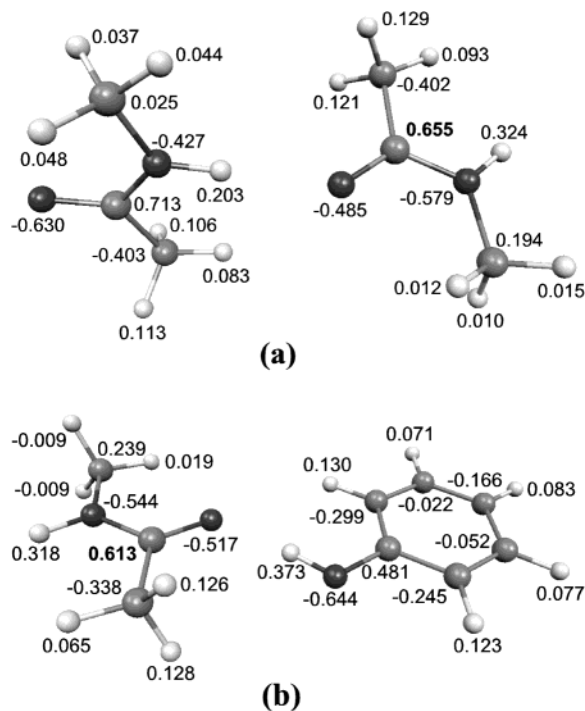


**Figure 3.** Calculated atomic charges in (a) self-associated *N*-methylacetamide dimer and (b) *N*-methylacetamide-phenol complex.

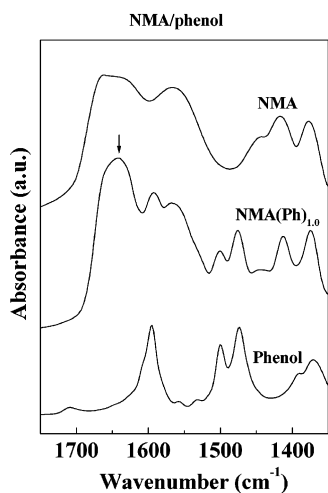


**Figure 4.** FTIR spectra of *N*-methylacetamide, phenol, and *N*-methylacetamide-phenol complex at 1350–1750  $\text{cm}^{-1}$  region. Amide I band is marked with an arrow.

**Table 2. Calculated Atomic Charges of *N*-methylacetamide as a Hydrogen Bonding Acceptor in Dimer and in its Complex with Phenol**

atom	charge in dimer	charge in complex
C1	0.655	0.613
O2	-0.485	-0.517
N3	-0.579	-0.544
H4	0.324	0.318
C5	0.194	0.239
H6	0.010	-0.009
H7	0.015	-0.009
H8	0.012	0.019
C9	-0.402	-0.338
H10	0.093	0.065
H11	0.129	0.128
H12	0.121	0.126

4 shows FTIR spectra of the studied oligomers in the 1350–1750  $\text{cm}^{-1}$  wavenumber range. In pure NMA, a

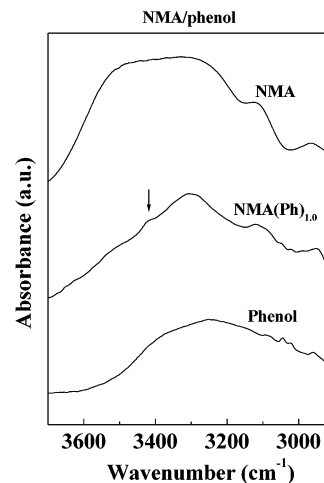


**Figure 5.** FTIR spectra of *N*-methylacetamide, phenol, and *N*-methylacetamide-phenol complex at 2900–3700  $\text{cm}^{-1}$  region.

split band is observed at the amide I region, having peaks at 1662 and 1634  $\text{cm}^{-1}$ . The latter one is attributed to the characteristic C=O stretching vibration (self-associated), whereas the peak at 1662  $\text{cm}^{-1}$  is assigned to an interaction between low-energy absorption modes and other amide bands or to a Fermi-resonance between some amide fundamentals.<sup>29</sup> A second characteristic mode of amides known as amide II band is observed at 1568  $\text{cm}^{-1}$  in pure NMA. Upon complexation with phenol, the intensity of the amide I fundamental increases considerably and the peak shifts to 1640  $\text{cm}^{-1}$ . The amide II band is found at 1564  $\text{cm}^{-1}$  in complex and its intensity remains essentially unchanged compared to the spectrum of pure NMA. These changes in the amide I and amide II regions suggest that self-association of NMA molecules is replaced by (stronger) hydrogen bonding between the carbonyl group and phenol, which supports the calculations.

N–H stretching and O–H stretching vibrations (2900–3700  $\text{cm}^{-1}$  region) provide further information on complexation (Figure 5). Pure NMA shows a broad amide A band between 3300 and 3500  $\text{cm}^{-1}$ , which is caused by the self-associated (3300–3400  $\text{cm}^{-1}$ ) and free (about 3500  $\text{cm}^{-1}$ ) amide N–H stretching vibrations.<sup>29</sup> Phenol, on the other hand, shows a broad O–H stretching band with peak at 3520  $\text{cm}^{-1}$  and a shoulder at about 3380  $\text{cm}^{-1}$ , originating from the phenol multimers ( $n = 2, 3, \dots$  etc.) with hydrogen bonding linkage between the monomers. A free O–H stretching band at 3600–3650  $\text{cm}^{-1}$  is not observed, which shows that the majority of the phenol molecules are self-associated.<sup>30</sup> Upon complexation between NMA and phenol, some changes take place. First, the intensity of the free amide N–H stretching band of NMA at 3500  $\text{cm}^{-1}$  decreases, which indicates that hydrogen bonding density is higher in the case of the NMA–phenol complex compared to pure NMA. Second, a shoulder is formed at 3420  $\text{cm}^{-1}$ , which we assigned to the O–H stretching vibrations of phenol hydrogen bonded with NMA. These findings combined with the calculations suggest a hydrogen bonding

(29) Herrebout, W. A.; Clou, K.; Dessey, H. O. *J. Phys. Chem. A* **2001**, *105*, 4865.

(30) Silverstein, R. M.; Bassler, G. C.; Morrill, T. C. *Spectrometric Identification of Organic Compounds*; John Wiley & Sons: USA, 1991.

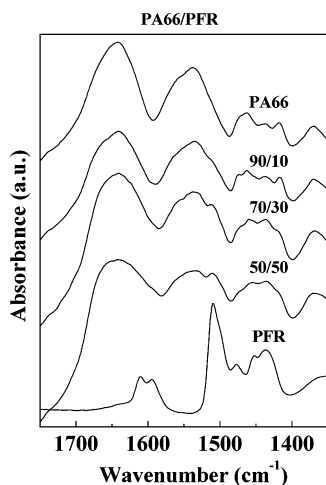


**Figure 6.** FTIR spectra of polyamide 66-phenol formaldehyde resin blends at 1350–1750  $\text{cm}^{-1}$  region.

between a carbonyl oxygen of NMA as a hydrogen bonding acceptor and a hydroxyl group of phenol as a donor.

FTIR analysis was also carried out for the polymeric blend of PA66 and phenol formaldehyde resin to study hydrogen bonding in the macromolecular system. Similar to the case of the model compound system of NMA and phenol, we have investigated the spectral changes at the carbonyl and amine/hydroxyl regions. Figure 6 depicts FTIR spectra of PA66-PFR blends as well as those of neat PA66 and PFR at the 1350–1650  $\text{cm}^{-1}$  region. Neat PA66 has an amide I band at 1640  $\text{cm}^{-1}$  and amide II band at 1537  $\text{cm}^{-1}$ , originating from C=O stretching and N–H bending vibrations, respectively. Upon blending with PFR, the relative intensity of the amide I peak decreases at first (until 10% of PFR), after which an increase of the intensity with a simultaneous peak broadening is observed. Broadening of the amide I band to lower frequencies may be partly due to the increasing proportion of phenolic resin (superposition), since PFR gives distinct absorptions at 1610 and 1595  $\text{cm}^{-1}$ , but it can be considered if this is also a sign of a new hydrogen bonding between carbonyl groups of PA66 and PFR. More evidence of the complexation is obtained by also analyzing higher frequencies of the spectra (Figure 7). Neat PA66 shows N–H stretching vibrations (amide A) at 3307 and 3500  $\text{cm}^{-1}$ , reflecting self-associated and free amide functionalities, respectively. Pure PFR shows a broad band with a peak at 3380  $\text{cm}^{-1}$  and is assigned to self-associated hydroxyl groups. In blends of PA66 and PFR, intensities of the free and self-associated N–H stretching bands decrease and the amide A band broadens towards lower frequencies. Additionally, there emerges a new peak at 3400  $\text{cm}^{-1}$ , which may originate from newly hydrogen-bonded O–H. Though the spectral changes at the amide I and amide II regions in PA-PFR blends were not as clear as in the case of model compounds, we suggest that the findings together with the quantum chemical calculations demonstrate a hydrogen bond formation between carbonyl groups of PA66 and PFR.

Differential scanning calorimetry (DSC) has been successfully used to study the morphological changes upon blending of polyamides and phenolic resins.<sup>15,16,19</sup> In this work DSC was used to study glass transition

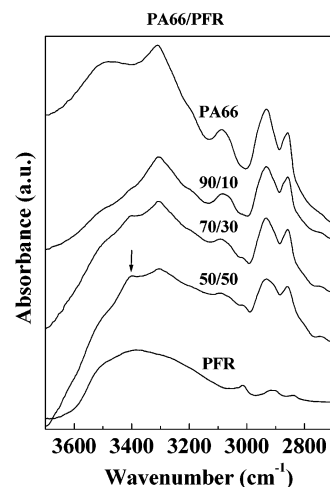


**Figure 7.** FTIR spectra of polyamide 66-phenol formaldehyde resin blends at 2900–3700  $\text{cm}^{-1}$  region.

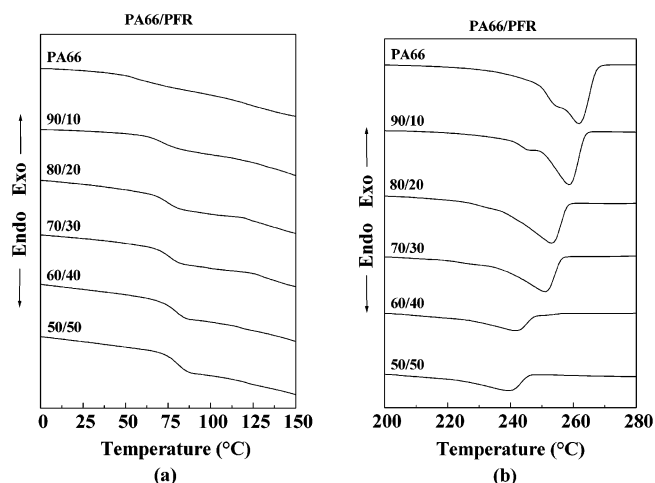


**Figure 8.** DSC thermograms of polyamide 66-phenol formaldehyde resin blends at (a) 0–150  $^{\circ}\text{C}$  region and (b) at 200–280  $^{\circ}\text{C}$  region.

**Table 3.**  $T_g$ ,  $\Delta T_g$ , and  $T_m$  of the Studied Blends at Different Ratios of PA66/PFR

sample	$T_g$ , $^{\circ}\text{C}$	$\Delta T_g$ , $^{\circ}\text{C}$	$T_m$ , $^{\circ}\text{C}$
PA66	56	0	261
95/5	67	10	261
90/10	72	14	259
80/20	74	14	256
70/30	75	13	251
60/40	79	15	241
50/50	80	14	243
PFR	77	0	–

temperatures ( $T_g$ ) and melting points ( $T_m$ ) of the blends, to analyze the miscibility of the components at different blend compositions. Figure 8a presents DSC scans of the PA66/PFR blends at 0–150  $^{\circ}\text{C}$ , showing a glass transition increase upon blending, and Figure 8b shows the DSC curves at the 200–280  $^{\circ}\text{C}$  temperature range. Observed  $T_g$  and  $T_m$  temperatures are given in Table 3, as well as the deviation of the obtained  $T_g$  from the calculated, weight average values according to definition:<sup>16</sup>

$$\Delta T_g = T_g - (\omega_a T_{ga}^0 + \omega_b T_{gb}^0) \quad (1)$$

where  $\omega_i$  is the weight fraction and  $T_{gi}^0$  is the glass transition temperature of the component  $i$ . A single  $T_g$

## PA66/PFR

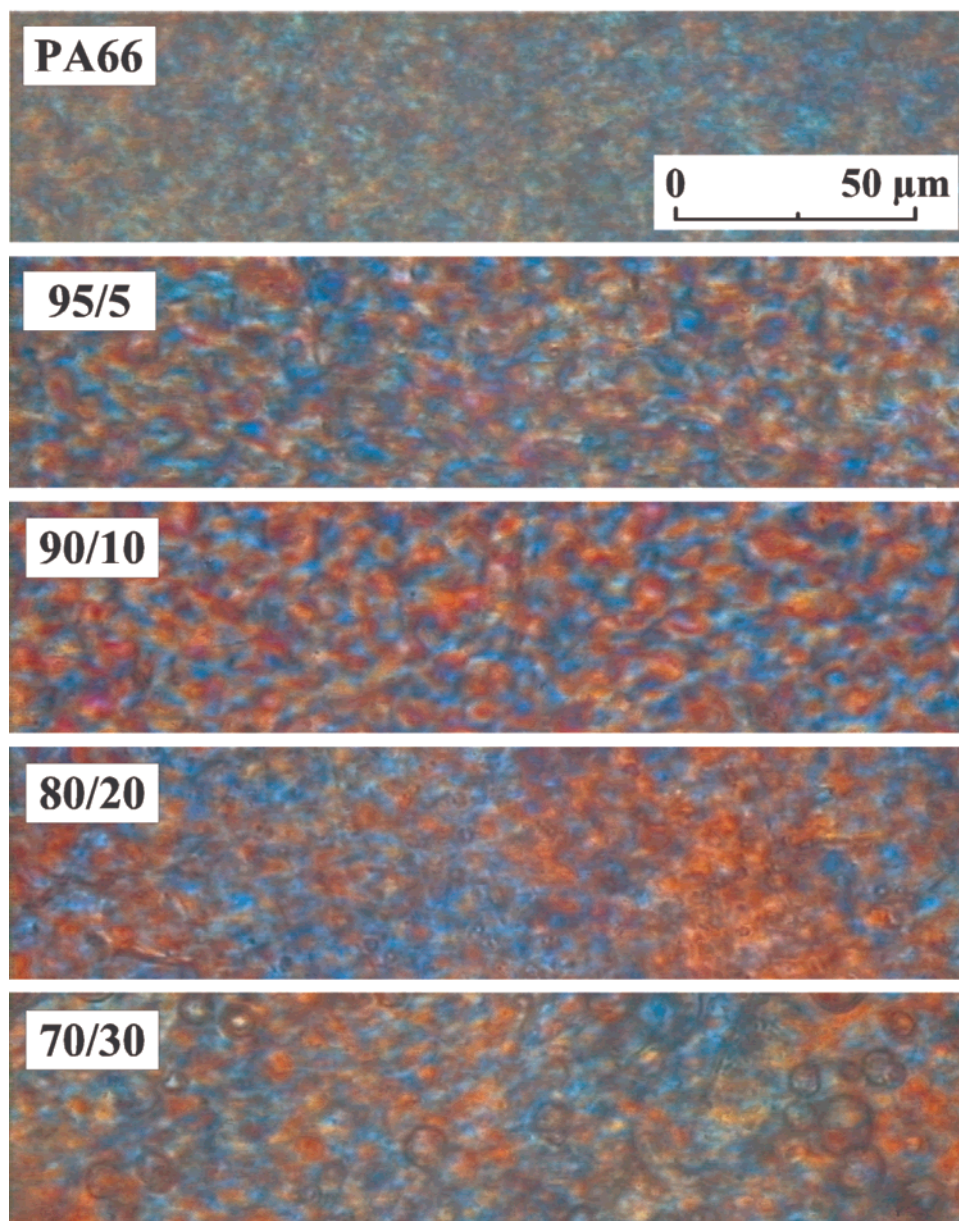


**Figure 9.** Cross-polarized optical micrographs of polyamide 66-phenol formaldehyde resin blends.

value is obtained for all blends, which implies that PA66 and PFR are miscible in the studied composition range. Additionally, the glass transition temperature  $T_g$  increases with increasing PFR content, which has also been observed in previous studies with PA6-phenolic resin blends.<sup>16,19</sup> It can also be noted that the deviation of the glass transition temperature of the blends from the weight average values is strongly positive, which has been observed in several thermoplastic-PFR blend systems.<sup>5,6,31</sup> The phenomenon is explained by considering the formed hydrogen bonds between PFR and polyamide as physical cross-links, which form a network and lead to an increase of the  $T_g$ . On the other hand, Figure 8b shows that melting temperature depression is observed as the PFR content increases. This reflects a strong interaction between the blend components.<sup>19,32</sup> These observations support the results of the FTIR

study, indicating that a strong intermolecular hydrogen bonding between PA66 and PFR results in miscible blends.

Finally, morphology of the blends was studied by using microscopic methods. First, an optical microscope was used to analyze whether the blends are birefringent under a polarization lens. Optical micrographs of PA66-PFR films with different phenolic resin contents are presented in Figure 9, showing that all samples are birefringent. A prominent feature is that the morphology becomes coarser with spherulite type structure as phenolic resin is added, which was also observed in recent studies with poly( $\epsilon$ -caprolactone)-PFR<sup>11</sup> and PA6-PFR<sup>17</sup> blends. This phenomenon indicates that PFR is not a typical nucleation agent, since in such a case it would be expected that the spherulite diameter would

(31) Kwei, T. K. *J. Polym. Sci., Polym. Lett. Ed.* **1984**, *22*, 307.

(32) Flory, P. J. *Principles of Polymer Chemistry*; Cornell University Press: Ithaca, New York, 1953.

## PA66/PFR (70/30)

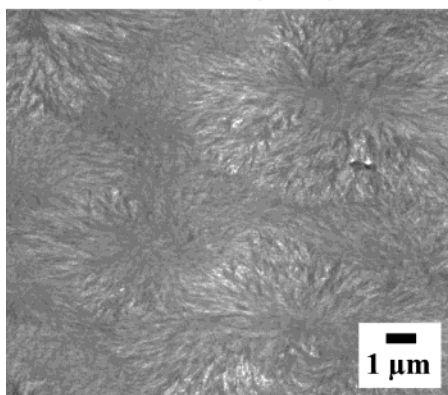


**Figure 10.** Transmission electron micrographs of polyamide 66-phenol formaldehyde resin blend, showing detailed spherulitic structure.

decrease and nucleation density increase. The phenomenon can also be seen by transmission electron microscopy analysis, which was used to study a blend including 30 wt % of phenolic resin (Figure 10) showing PFR induced spherulite growth in PA66. It should be noted that there was no interspherulitic, phase-separated PFR phase present, which was also indicated by the single  $T_g$  temperatures in DSC. However, it is known that PFR is an amorphous material and is rejected from the crystalline lattice during the crystallization process of the polyamide counterpart, as indicated by the SAXS patterns of PA6-PFR blends.<sup>19</sup> Thus, it can be concluded that PFR induces the spherulite growth rate, but is itself probably located in the amorphous phase in blends with PA66.

### Concluding Remarks

Blends of polyamide 66 with oligomeric phenol formaldehyde resin were studied by molecular modeling for the model compounds and experimentally by FTIR, DSC, and microscopic analyses. Modeling for the simple, small molecular weight model compounds showed that in a minimum energy state there exists a hydrogen bonding between the carbonyl oxygen of *N*-methylacetamide (model for polyamide) and the hydroxyl group

of phenol (model for phenolic resin). The calculated complexation energy in the NMA-phenol complex was  $-38$  to  $-39$  kJ/mol (depending on the method), whereas in NMA dimer it was  $-26$  to  $-31$  kJ/mol and in phenol dimer  $-19$  to  $-24$  kJ/mol. This indicates that there exists a strong physical interaction between NMA and phenol exceeding that of the NMA and phenol dimers. Second, the calculations showed that water molecules may replace amide-amide hydrogen bonds with amide-water hydrogen bonds, since the interaction energies were at the same level. The interaction energy in the NMA-phenol complex was higher than in NMA dimer, phenol dimer, or in the NMA-water complex, indicating a more stable structure. These results provide an explanation for the decreased water absorption in polyamides upon blending with phenolic resins, which has been observed in earlier studies. FTIR spectroscopy supports the calculations, since the shifts and intensity changes also suggest hydrogen bond formation between a carbonyl group of amide and a hydroxyl group of phenol, both in model compounds and in polymer blends. The single  $T_g$  value of the blends in DSC demonstrates miscibility within the studied composition range (up to 50 wt % of PFR in PA66). Also, phenolic resin seems to induce spherulite growth, as indicated by the studies with an optical microscope and a transmission electron microscope. Concluding, blending of PA66 with oligomeric phenol formaldehyde resin results in miscibility due to a physical bonding and offers a route to achieve new property combinations in this commodity thermoplastic polymer.

**Acknowledgment.** Prof. J. Karger-Kocsis is gratefully acknowledged for help in understanding the morphology of the blends. J. Poch Parramon of Engineering Office ATK, Germany, is sincerely thanked for collaboration, discussions, and support. Finnish IT Center for Science (CSC) is acknowledged for computer resources. The research is financially supported by the European Commission under Marie Curie Fellowships program, contract number G5TR-CT2001-00052.

CM0401591